Hyperspectral microscopy

Does the hyperspectral signature of a muscle of mouse indicate its ageing ?

Authors
Quentin Douzery
Alexia Ghozland

January,13 2022

Abstract

First used in space missions, hyperspectral imaging is part of the microscopy evolution, for ten years. *RESTORE* tries to use it as a way to detect the ageing of humans. No studies have been performed for now, and the first investigations are ongoing. We studied muscles of mice: the aim was to determine if there were differences between the hyperspectral signatures of old mice and young mice. We transformed our images with segmentation tools in order to compute the normalized mean spectrums and the normalized median spectrums of the mice. The first results tended to show that there is not a significant difference, but the study has to be continued on more samples in order to be reliable. This work lays the foundations for other projects that will study the images in more detail, focusing on the outliers of the images.

Keywords : Hyperspectral imaging, image segmentation, spectrum

Contents

1 Introduction

Standard vision systems are based on human vision by exploiting the three colors red, green, blue (RGB). Mainly used in planetary exploration, hyperspectral imaging is a new microscopy technology [1] which allows the acquirement of the complete spectral signature for each image's pixel, regardless of their color. Instead of simply measuring light intensity, we can evaluate the emission spectrum (from three to several hundred channels) of a sample at each point of a two-dimensional plane or three-dimensional space. This technology is able to distinguish the full color spectrum in each pixel (for a two-dimensional object) or voxel(for a three-dimensional object). Thus, hyperspectral imaging detects both spatial and spectral information from an object. Hyperspectral imaging would offer new avenues for detecting ageing, as it is a non-destructive and a non-contact method.

Thanks to this technique, the geroscience and rejuvenation center *RESTORE*, provided us with young and old mice muscle images. Based in Toulouse, one of the research center's questions is: do spectral signatures of the mice samples allow to distinguish their condition?

In order to answer to this question, we segment both young and old muscle images with the softwares *Ilastik* and *Python*: regions of muscle pixels are distinguished from non muscle ones. Then, we visually compare a young muscle spectrum against an old one to analyse if there are any differences. We finally conduct a statistical test to deeper examine how different each mice sample is, regarding its condition.

2 Scientific context

2.1 Research about ageing

Ageing reflects by multiple ways: visually by appearance of wrinkles, and in a less visible way by loss of skeletal muscle mass [2]. But, not only these changes have a role in ageing-related muscle dysfunctions. There are also other factors, as the emergence of fibrosis or muscle tissue composition changes. Among our cells, there are certain called adipocytes that manage fats storage. With age, an accumulation of adipocytes can occur.

Thanks to certain molecules involved in cell metabolism, biological tissues show autofluorescence. When excited by external illumination sources, these tissues emit light. Hyperspectral camera is one of the illumination source that uses this characteristic, allowing us to identify the ageing-related changes mentioned.

2.2 What is hyperspectral imaging

As each individual has a unique fingerprint, each pixel of an image has its own spectral signature. Hyperspectral imaging is one of spectral analysis techniques that allows the identification of materials or the detection of processes on an image, thanks to the spectral signature of the pxiels. This technique divides an image into a large number of narrow and contiguous spectral bands across a wide range of wavelengths, beyond the visible. This range can start with the visible spectrum and end in the near-infrared (IR). Hyperspectral technology reveals object's properties and characteristics that are not otherwise apparent.

Hyperspectral imaging is related to multispectral imaging and both are more accurate than standard three bands vision imaging (RGB). The RGB identification capability is minimal as the camera is limited to three color bands [3]. Hyperspectral and multispectral imaging capture wavelengths from $400nm$ to $1100nm$. These two techniques are beneficial for the agriculture (e.g. water stress detection), environment (e.g. detection and monitoring of pollution), astronomy (characterization of stars), but also for culture (analysis and restoration of art works). However, they represent two distinct imaging practices.

The figure below (Fig. 1) illustrates the main difference between multispectral and hyperspectral imaging [4]:

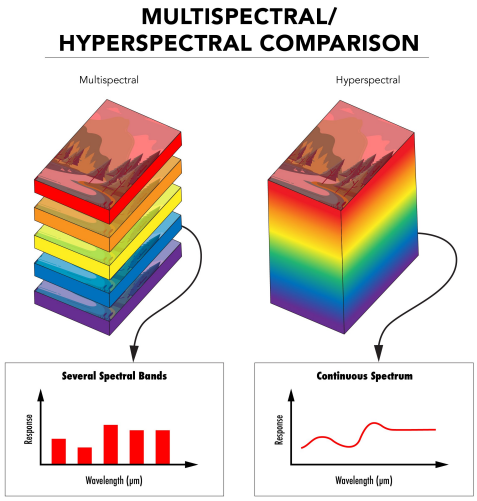

Figure 1: Multispectral versus hyperspectral imaging

While multispectral imaging generally refers to spaced spectral bands, hyperspectral imaging measures continuous spectral bands. The latter deals with narrow spectral bands over a continuous spectral range, producing the spectral signature of all pixels in the scene. Multispectral imaging deals with several images at discrete and somewhat narrow bands. Thus, hyperspectral imaging gives higher spectral resolution. Hyperspectral imaging avoids preparing antibody labelling and replaces scanning probe microscopy. It is based mainly on intrinsic tissues properties.

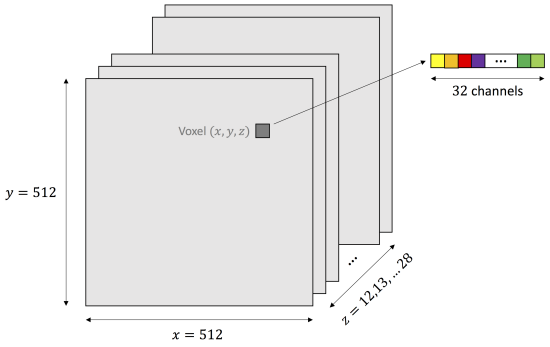

Figure 2: Diagram of an hyperspectral image

In our report, hyperspectral images are three-dimensional, represented by the coordinates (x, y, z), with z differing from image to image. An image is composed of voxels, equivalent of pixels in $2D$. Each voxel has 32 channels and each one has an intensity value.

Our images have a $(512, 512, z)$ shape. An hyperspectral sensor captured an emission spectrum from $410nm$ to $690nm$, every $8.9nm$ corresponding to the 32 channels. *RESTORE* provides us with some images to work with: old and young muscles images of different mice, for three different excitation wavelengths: $740nm$, $780nm$, and $820nm$.

3 Materials and methods

3.1 Segmentation of the images

On our hyperspectral images, we observe two types of sections: sections that correspond to muscle, and sections that are everything but muscle. Thus, the first point was to segment the images, i.e. to determine which section corresponds to muscle and which does not. For that, we needed to determine if each voxel belongs to a muscle section or not.

The tool we used in this way is a software called *Ilastik*. The principle was the following:

1. Chose the features that will be used to segment the image. Here, we used the feature *Color/Intensity* as the differences between muscle and non muscle sections mostly rely on the fluorescence of the voxels (so on their intensity in a way).
2. Select by hand on the image some muscle sections (light), and some non muscle sections (dark). During this step, we selected sections only where we were **sure** it was muscle/non muscle.
3. Let the software works: it is a machine learning algorithm, which trains itself on the sections we selected, and predicts the affiliations to muscle section for all voxels which were not selected. Here, it is a random forest algorithm.

At the end of the process, we thereby obtained a class for each voxel: a voxel belonging to a muscle section got a 1 value, while the others were set to 0. As a result, the segmented image had the following size: $(512 \times 512 \times z)$, where z is the z coordinate of the raw image (the one we segmented). Thus, we had no more channels. See Figure 3 the difference between a raw image and the segmented image associated. As a convention, a voxel which has a 1 value is displayed in white, and a voxel which has a 0 value is displayed in black. Note that the images below are displayed for a given z and a given channel.

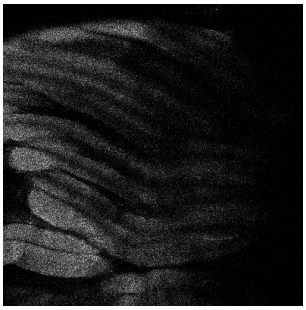

(a) Raw image, given z and given channel

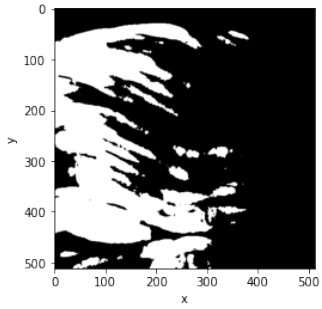

(b) Segmented image, given z

Figure 3: Difference between a raw image and the associated segmented image

We used two different tools to visualize the images : *Fiji* or *Python* (with the *Pyplot* library).

3.2 Mathematical morphology

Second, we used mathematical morphology, in order to complete the segmentation. It consists in a set of operators that transform a binary[1] image according to its size, its shape, or its connectivity. The two most basic transformations are the following: **erosion** and **dilatation**. We recall that these operations are done on two-dimensional images.

[1] Actually, it was originally developed for binary images, but then extended to coloured images or grayscale functions.

3.2.1 Erosion

An erosion is a basic morphological operator: it needs two inputs (the original image and a kernel), and gives an output (the eroded image). The kernel is a shape (a square, a circle, a diamond, etc.) of a given size (5×5 pixels or 20×20 pixels for example) that will perform the transformation.

The kernel slides through the whole image. At each step, if a pixel under the kernel is equal to 0 (we recall that we have a binary image, so all the pixels are just equal to 1 or 0), then all the pixels under the kernel are set to 0. Rewording, a pixel under the kernel stays equal to 1 if and only if all the pixels under the kernel are equal to 1.

As a result, the pixels near the boundary of the figure (i.e. the shape formed by all the pixels equal to 1) are discarded. Thus, the figure becomes thinner, and the noise[2] disappears. The final thickness then depends on the size and the shape of the kernel. See Figure 4 for an illustration [5].

(a) Original image (b) Image after erosion

Figure 4: Illustration of an erosion in mathematical morphology

3.2.2 Dilatation

The principle of the dilatation is very similar to the erosion's one. From an original image and a kernel, we obtain an output image called the dilated image. But here, the kernel does the opposite transformation: at each step, if only one pixel under the kernel is equal to 1, then all the pixels under the kernel are set to 1.

As a result, the white region of the figure increases, proportionally to the kernel's size. See Figure 5 for an example [5].

(a) Original image (b) Image after dilatation

Figure 5: Illustration of a dilatation in mathematical morphology

[2]The noise on an image are the little groups of pixels equal to 1 that are far from the figure(s).

3.2.3 Opening

We finally get to the important point: the opening. Now we have seen what are an erosion and a dilatation, it is very basic. An opening is just an erosion followed by a dilatation. The goal is to remove all the noise (with the erosion), while keeping intact the general appearance of the figure (with the dilatation, which recovers the sections the erosion discarded).

In our case, we apply an opening on our image in order to be sure that all the 'muscle' voxels really correspond to muscle sections of the image. In other words, we want to remove all the noise of the image that could distort the analysis we will do. Below, we show the result of the opening on one of our segmented images.

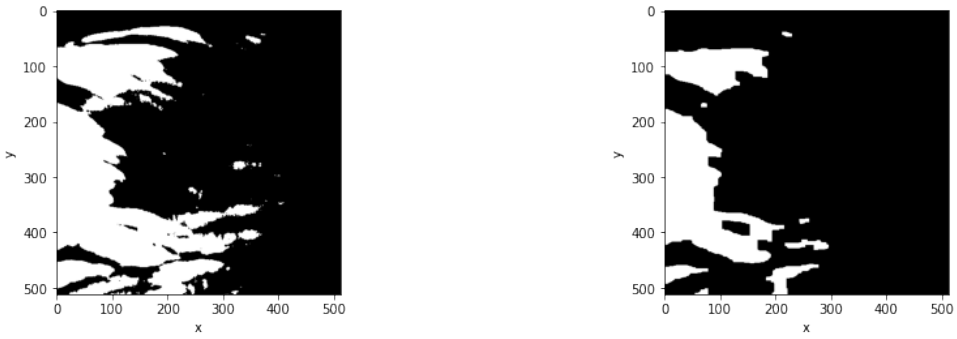

(a) Segmented image

(b) Image after opening and additional erosion

Figure 6: Illustration of an opening in mathematical morphology

It should be noted that we here performed an additional erosion after the opening, always in order to be sure that 'muscle' voxels really correspond to muscle. For the opening, we use a 20×20 square kernel; for the additional erosion, we use a 15×15 square kernel.

As mentionned before, those morphological transformations are done on two-dimensional images. In this way, our images being three-dimensional, we apply the operators for each different z coordinate on one given image.

3.3 Spectrum analysis

Third, we used both our raw images and segmented images in order to compare the muscles of old and young mice. We recall the main feature of each type of image:

- The raw image contains the fluorescence value for each channel of each voxel.
- The segmented image tells us if a voxel belongs to a muscle section.

Thus, for a given channel, multiply the raw image by the segmented image gives the fluorescence value (of the considered channel) of each muscle voxel. From that, we retrieved the mean spectrum and the median spectrum of a given image. The principle is as follows:

- For each channel, we computed the mean value of all muscle voxels. Then, the mean spectrum is denoted as the array which contains the mean values of all channels.
- Computing the median spectrum was very similar: we just had to compute the median[3] value of all muscle voxels for every channel. It should be noted that the median often describes a dataset in a better way than the mean, as it is not sensible to extreme values.

The last step was normalizing the spectrums, since the measured fluorescence values depend on many parameters: the time of exposure, the sensitivity of the sensors, or the way to prepare the images. For example, a larger image is more likely to generate fluorescence if there is a wrong focus. As a result, we needed to divide each value of the spectrums by the maximum value of each spectrum. Thus, we obtained spectrums at the same scale: then, all was about comparing the values of an old muscle with a young one, channel by channel.

[3]The median is the value that separates the higher half from the lower half of a sorted data sample.

3.4 Mann-Whitney U test

Statistical hypothesis testing is used to determine a conclusion from two different hypothesis. Mann-Whitney U test is part of this testing method.

Supposing two independent samples X and Y, with a minimum size of four (but both samples potentially have different sizes). This test is based on rank, i.e. the order in which the observations of the two samples appear when they are combined and sorted. It tests the hypothesis $H0$: the probability that an observation from X is greater than an observation from Y is equal to the probability that an observation from Y is greater than an observation from X. In other words, it tests if the distributions of both samples are the same.

By counting values from X which are greater than those from Y in the sorted list, we obtain u_1. By doing the same respectively with Y values greater than X values, we obtain u_2. Then, by adding u_1 and u_2, we get the Mann-Whitney statistic, denoted by U. It is the value of U that determines if the samples follow the same distribution. If U exceeds a threshold, then we reject the hypothesis $\mathcal{H}0$.

The *p-value* also allows us to decide if we reject the hypothesis $\mathcal{H}0$ or not. It represents the probablity to reject $\mathcal{H}0$ wrongly i.e. even though $\mathcal{H}0$ is true. Here are the different cases:

- $p \leq 0.01$: very strong presumption against the $\mathcal{H}0$;
- $0.01 < p \leq 0.05$ strong presumption against the $\mathcal{H}0$;
- $0.05 < p \leq 0.1$ weak presumption against the $\mathcal{H}0$;
- $p > 0.1$: no presumption against the $\mathcal{H}0$.

In our case, we wanted to compare distributions between two samples, a young one versus an old one. The samples were composed of the fluorescence value for all muscle voxels for a given channel (from 1 and 32).

4 Results and discussion

We applied the methods described above on 8 images with excitation wavelength of $740nm$: half corresponds to muscle from old mice, the other to muscle from young mice. For each set of 4 images, we have:

- 2 different subjects.
- 2 different viewpoints for each subject.

The names of the images are denoted as follows :

Age (old or young)	Subject (n°)	Section	Name
Young	1	1	*young*_1_1
	1	2	*young*_1_2
	5	1	*young*_5_1
	5	2	*young*_5_2
Old	2	2	*young*_2_2
	2	3	*young*_2_3
	6	3	*young*_6_3
	6	4	*young*_6_4

Table 1: Overview of the different images

4.1 Spectrum analysis

4.1.1 Muscle sections

As we mentioned before, we first computed the normalized mean and median spectrums of the muscle sections of the images. In order to have a visual representation, we ploted the normalized mean and median fluorescence of the images depending on the channels.

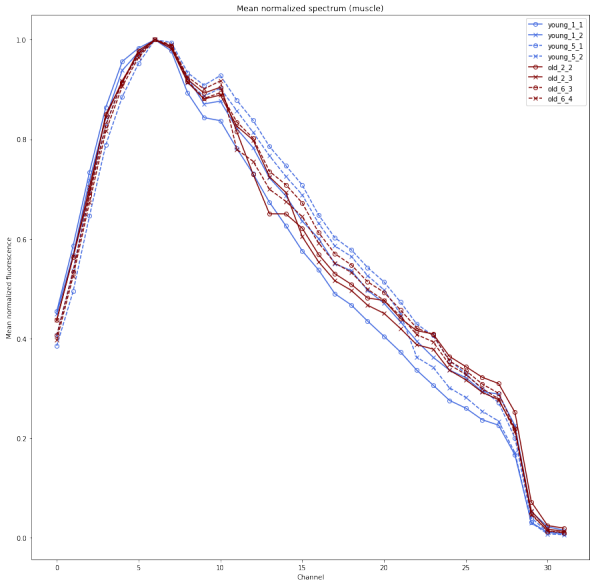

Figure 7: Normalized mean spectrums for the muscle sections of the images

First, let us describe the general aspect of the spectra. We observe that the 8 spectrums follow a similar curve: the first channel is around 0.4, then the values increase to a peak on the 7^{th} channel, and finally they decrease until 0 on the last channel.

If the spectrums are very close on the first 9 channels and on the 4 last ones, it is not the case between. But the essential point is that the differences between channels 10 and 28 are very faint: the spectrums of the old mice merge with the ones of the young mice. Thus, there is not a particular tendency for the "old spectra" or for the "young spectra". We may observe some spectrums that are quite different (the *young_1_1* between channels 15 and 25 for example), but it is too poor to see a pattern in it.

We now plot the normalized median spectra.

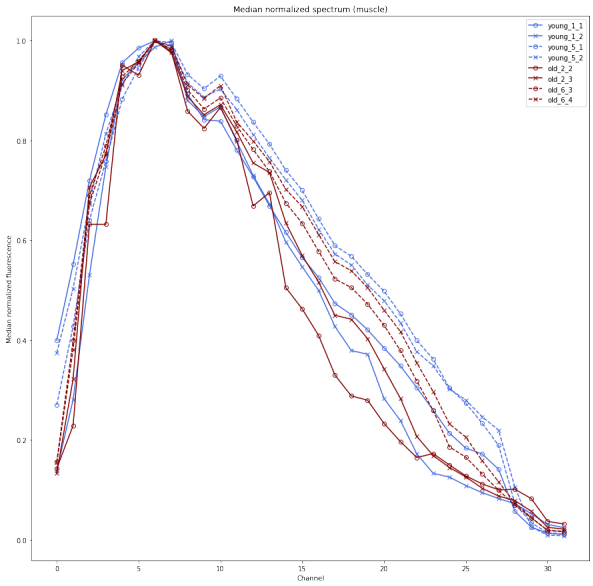

Figure 8: Normalized median spectrums for the muscle sections of the images

The general aspect of the median spectrums is very similar to the aspect of the mean spectra. We do not observe differences for the first channels, but some appear from the 10^{th} one. The curves are well separated (they do not cross each other), but again, we cannot see a tendency for the spectrums of the old mice or the spectrums of the young mice.

Thus, the results of the two graphs above tend to show that there is not a difference between the spectral signature of muscles of old mice and the spectral signature of muscles of young mice. So we analyse the spectrums of the non muscle sections, applying the same principle described in Section 3.3 for non muscle sections of the images.

4.1.2 Non muscle sections

First, we display the normalized mean spectra. The general aspect is the following: the first channel is around 0.5, it reaches the maximum value around the 7^{th} channel, then it decreases slowly to the 28^{th} channel, and it finally decreases suddenly to 0 at the end.

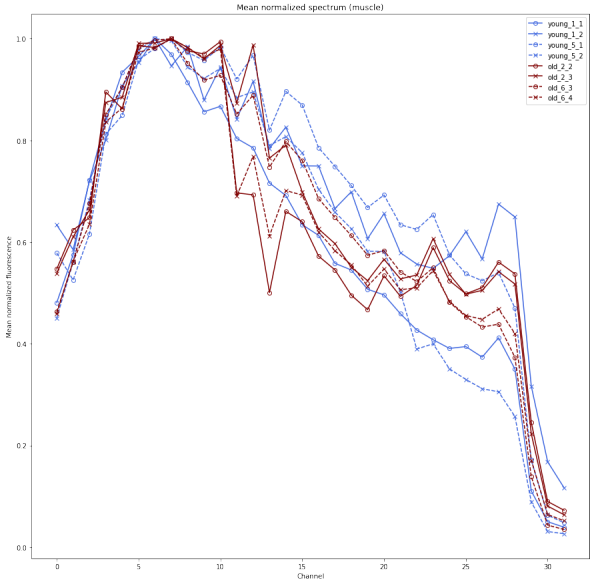

Figure 9: Normalized mean spectrums for the non muscle sections of the images

The 8 spectrums are very close until the 10^{th} channel. After, they become less smooth, with many variations. It is impossible to see a tendency between all the spectra, and even more to see a difference between the spectrums from the old mice and the spectrums of the young mice.

The last figure represents the normalized median spectrums of the non muscle sections.

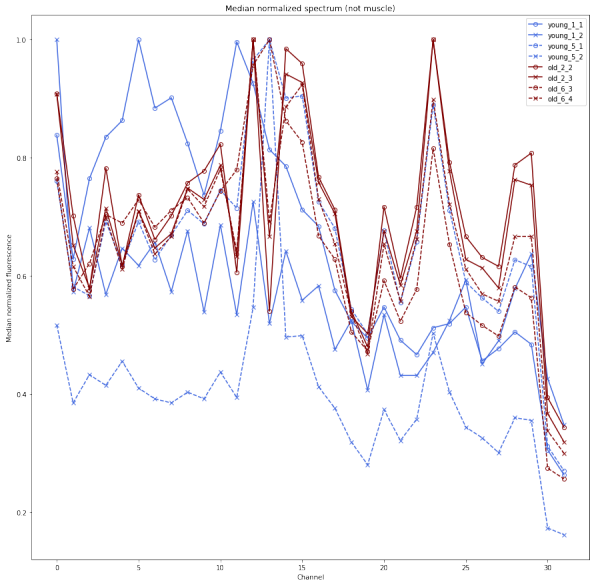

Figure 10: Normalized median spectrums for the non muscle sections of the images

The spectrums are very different from each other, whether it be in the general aspect (the sample *young_5_2* has much smaller values), or in the variations from one channel to another (the spectrum of the *young_1_2* is not smooth at all). The only tendency we could observe is that the spectrums of the young mice seem to have lower values between channels 20 and 25. But it is not the case for all the spectra, as the one of the sample *young_1_1* is very close to the spectrums of the old mice between these channels.

Thus, it is again hard to see a real difference between the spectrums of the old mice and the spectrums of the young mice.

4.2 Mann-Whitney U test

Since we do not distinguish global differences between the spectral signatures, we tried to deeper analyse muscle voxels fluorescence, for each channel. First, we combined histograms of an old and a young mouse for each channel, showing muscle voxels' density regarding fluorescence.

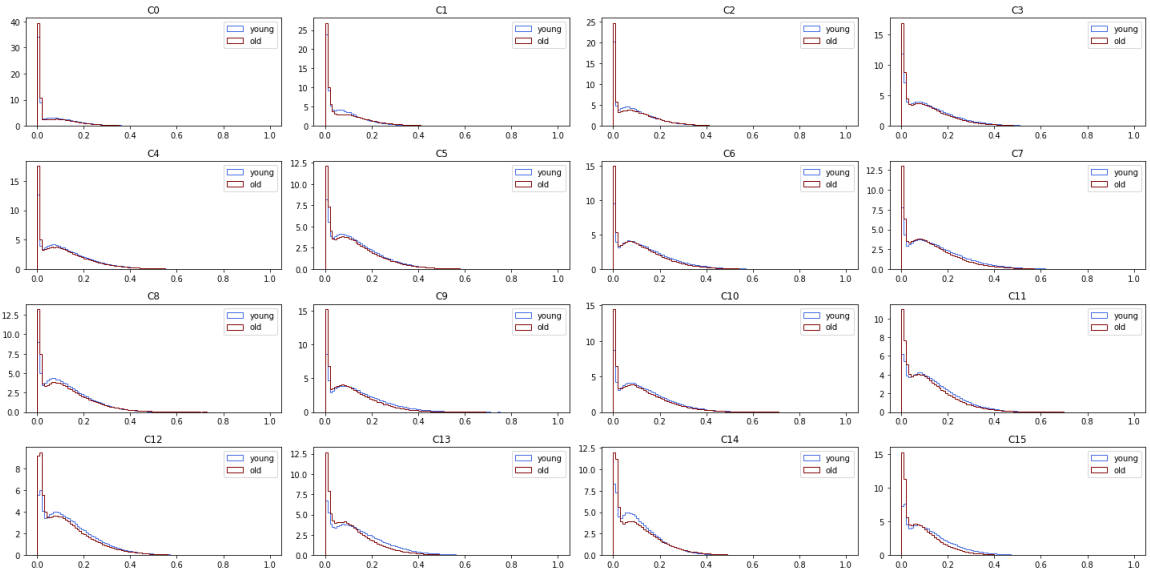

Figure 11: Muscle voxels distribution, regarding fluorescence, in a young (blue) and an old (red) image from channel 0 to 15

The example above, shows the distribution of muscle voxels (in percentage), depending on the fluorescence (normalized) between a young mice muscle and an old one. Even if we can observe a very small difference for example at the 14^{th} channel, we do not globally notice very significant differences between red and blue histograms to conclude.

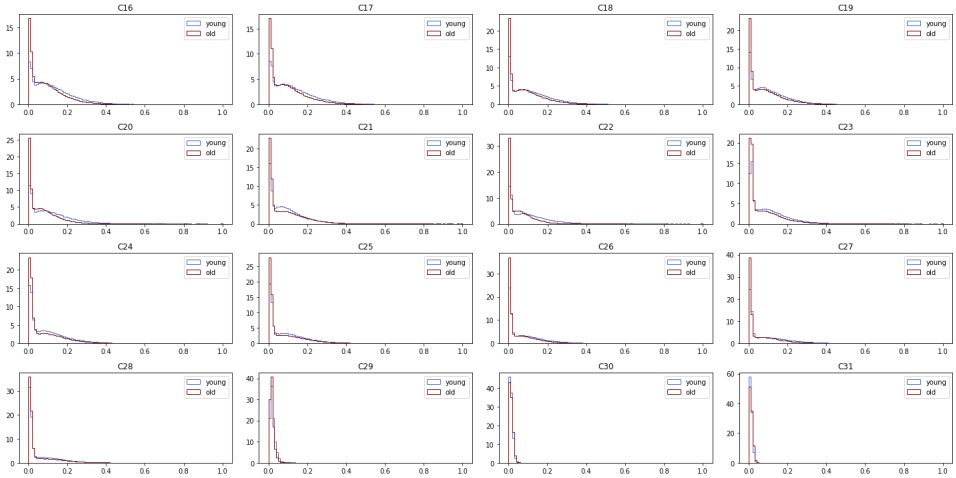

Figure 12: Muscle voxels distribution, regarding fluorescence, in a young (blue) and an old (red) image from channel 16 to 31

These 16 to 31 channel histograms are not really better, in terms of differences. It seems, for example on the channel 21 to be more muscle voxels for the young mouse.
Thus, we used the Mann-Whitney U test to determine if fluorescence value for all muscle voxels, for a given channel, was definitely different between an old and a young mouse, or not. We obtain *p-values* as $p = 0$ or $p < 0.01$: our young and old samples are different. However, we can express reservation about conditions for applying Mann-Whitney U.

4.3 Discussion

First, the number of observations in our samples is very huge (more than 200000 values for a given channel). The Mann-Whitney test is known to be efficient on small samples, but far less when the size increases. Here, we have so much values that the test will necessarily detect many differences (even if there is just 1% of the observations that are significantly different, it represents here 2000 observations), leading to these *p-values* of 0. Hence, the results are not reliable. And second, the observations of each sample are not independent, as they come from the same image, i.e. the same individual. Thus, the Mann-Whitney test was an interesting path to follow, but the acceptation conditions of the results are unfortunately not fullfilled.

But the Mann-Whitney test remains a solution to determine if there are differences. For example, we could apply it on the normalized median (or the normalized mean) values of a given channel, for different individuals (which here would be independent). But it supposes to have more mice, which is not the case here. The required number of mice to apply the Mann-Whitney test is: 4 old mice and 4 young mice [6]. This number of mice would also be the minimal number in order to properly analyse the graphes comparing the spectrums of the old and young mice (we recall that we obtained graphs with 2 old mice and 2 young mice in this report).

An other solution to implement the Mann-Whitney test could be to generate a random sub sample from each of our samples, in order to reduce the size of the samples and to have more independence. But it would probably lead to samples that are still too large to accept and validate the results.

One last possibility is to spot and analyse some outliers that are present on the images. These points manifest themselves being much brighter and colored. We did not work on this point during the project as we study the general structure of the images, but it could be an interesting path to study for future researches.

5 Conclusion

Our main goal was to deduce from muscle hyperspectral images of old and young mice if ageing detection is possible.

To do this, we first segmented our images to distinguish muscle and non muscle sections. Then, we did morphology operations on our segmented images to remove noise and reveal hidden muscle parts. Once image processing was done, we began our analysis by comparing our old and young spectral signatures, for muscle parts in the first place, and non muscle parts, then.

We did not find out significant differences between our old and young spectral signatures. We continued our analysis by using a Mann-Whitney U test in order to compare two samples : one about fluorescence values of muscle voxels of a young mouse, the other one about the old mouse. At first glance, we could conclude that our samples are significantly different. However, some limitations have to be taking into account : the number of observations in both samples is very huge and we do not have enough different individuals per condition.

Even if our analyses lead us to believe that we can not detect ageing with hyperspectral imaging, we are not so categorical. Indeed, **it would be interesting to apply our techniques with 4 young mice and 4 old ones**, in order to obtain reliable results. Another research opportunity is to deep analyse these bright points we can find on the images, which could have a considerable influence on *RESTORE*'s conclusions. For all these reasons, our current results should be interpreted and used with extreme caution.

References

[1] Telmo Adão, Jonáš Hruška, Luís Pádua, José Bessa, Emanuel Peres, Raul Morais, and Joaquim João Sousa. Hyperspectral imaging: A review on uav-based sensors, data processing and applications for agriculture and forestry. *Remote Sensing*, 2017.

[2] Rosaly Correa de Araujo, Michael O. Harris-Love, Iva Miljkovic, Maren S. Fragala, Brian W. Anthony, and Todd M. Manini. The need for standardized assessment of muscle quality in skeletal muscle function deficit and other aging-related muscle dysfunctions: A symposium report.

[3] Hyperspectral technology vs. rgb. `https://www.specim.fi/hyperspectral-technology-vs-rgb/`, 2020.

[4] Jaylond Cotten-Martin. Hyperspectral and multispectral imaging. `https://www.photonics.com/Articles/Hyperspectral_and_Multispectral_Imaging/a65595`, 2020.

[5] Opencv: Morphological transformations. `https://docs.opencv.org/3.4/d9/d61/tutorial_py_morphological_ops.html`.

[6] Jean-Yves Baudot. Test de mann-whitney. `http://www.jybaudot.fr/Inferentielle/mannwhitney.html`.